

NASA TECHNICAL MEMORANDUM

NASA TM X-64909

(NASA TM-X-64909) THE MEASUREMENT OF THE
SIZE DISTRIBUTION OF ARTIFICIAL FOGS (NASA)
43 p HC \$3.75 CSCL 04B

N75-20940

Unclas
G3/47 14705

THE MEASUREMENT OF THE SIZE-DISTRIBUTION OF ARTIFICIAL FOGS

By Adarsh Deepak, William C. Cliff, John R. McDonald,
Robert Ozarski, J. A. L. Thomson, and Robert M. Huffaker
Electronics and Control Laboratory

October 1974

NASA



*George C. Marshall Space Flight Center
Marshall Space Flight Center, Alabama*

TECHNICAL REPORT STANDARD TITLE PAGE

1. REPORT NO. NASA TM X-64909		2. GOVERNMENT ACCESSION NO.		3. RECIPIENT'S CATALOG NO.	
4. TITLE AND SUBTITLE The Measurement of the Size-Distribution of Artificial Fogs				5. REPORT DATE October 1974	
				6. PERFORMING ORGANIZATION CODE	
7. AUTHOR(S) Adarsh Deepak*, William C. Cliff, John R. McDonald**, Robert Ozarski†, J.A.L. Thomson††, and Robert M. Huffaker				8. PERFORMING ORGANIZATION REPORT NO.	
9. PERFORMING ORGANIZATION NAME AND ADDRESS George C. Marshall Space Flight Center Marshall Space Flight Center, Alabama 35812				10. WORK UNIT NO.	
				11. CONTRACT OR GRANT NO.	
				13. TYPE OF REPORT & PERIOD COVERED Technical Memorandum	
12. SPONSORING AGENCY NAME AND ADDRESS National Aeronautics and Space Administration Washington, D.C. 20546				14. SPONSORING AGENCY CODE	
15. SUPPLEMENTARY NOTES Electronics and Control Laboratory, Science and Engineering				*National Research Council Postdoctoral Research Associate **South Dakota School of Mines and Technology. †Wayne State University, Detroit, Michigan. ††Physical Dynamics, Inc., Berkeley, California.	
16. ABSTRACT The size-distribution of the fog droplets at various fog particle concentrations in the NASA-Ames Research Center fog chamber, Richmond, California, was determined by two methods: (1) the Stokes' velocity photographic method [1] and (2) using the active scattering particle spectrometer (Particle Measuring Systems Co., Boulder, Colorado) described in Reference 3. It is shown that the two techniques are accurate in two different ranges of particle size — the former in the radii range (0.1 μm to 10.0 μm), and the latter for radii greater than 10.0 μm . This was particularly true for high particle concentration, low visibility fogs.					
17. KEY WORDS			18. DISTRIBUTION STATEMENT Unclassified-unlimited <i>William C. Cliff</i>		
19. SECURITY CLASSIF. (of this report) Unclassified		20. SECURITY CLASSIF. (of this page) Unclassified		21. NO. OF PAGES 43	
				22. PRICE NTIS	

TABLE OF CONTENTS

	Page
INTRODUCTION	1
THE STOKES' VELOCITY PHOTOGRAPHIC METHOD	1
The Stokes' Law	1
The Range of Application of the Stokes' Law	2
Description of the Method	5
The Experimental Apparatus	5
A Settling Experiment with Fog Particles	9
Experimental Measurements and Results	13
Data Analysis	18
ACTIVE SCATTERING PARTICLE SPECTROMETER (ASPS)	
METHOD	20
Description of the Instrument	20
Particle Size Distribution, $n(r)$	22
DISCUSSION OF THE RESULTS	23
REFERENCES	35

LIST OF ILLUSTRATIONS

Figure	Title	Page
1.	Stokes' velocity versus radius	3
2.	Schematic illustration of the method	6
3.	Photograph of the experimental setup	7
4.	Schematic diagram of the photographic system	8
5.	Acetone and dry ice pump	8
6.	Fog chamber layout	10
7.	Injection of fog into test chamber	11
8.	Oscilloscope photograph (time scale: 1 sec = 0.5 cm)	13
9.	The chopping rate recorded on a chart recorder for: (1) a small pulley and two-blade chopper (chart speed = 5.0 cm/sec) and (2) a large pulley and a four-blade chopper (chart speed = 25.0 cm/sec)	14
10.	A photograph of the graph paper scale placed in the center plane of the slab of light	15
11.	Schematic of the horizontal cross section of the projected sheet of light	16
12.	A typical photograph of fog particles inside the chamber	17
13.	Optical system diagram for active scattering particle spectrometer	21
14.	Active scattering particle spectrometer probe	22
15.	Active scattering particle spectrometer data system and control console	23
16.	The size distribution $n(r)$ curves for a fog density level corresponding to a transmissometer transmittance of approximately 1 percent	26

LIST OF ILLUSTRATIONS (Concluded)

Figure	Title	Page
17.	The size distribution $n(r)$ curves for a fog density level corresponding to a transmissometer transmittance of approximately 3 percent	27
18.	The size distribution $n(r)$ curves for a fog density level corresponding to a transmissometer transmittance of approximately 10 percent	28
19.	The size distribution $n(r)$ curves for a fog density level corresponding to a transmissometer transmittance of approximately 15 percent	29
20.	The size distribution $n(r)$ curves for a fog density level corresponding to a transmissometer transmittance of approximately 30 percent	30
21.	The size distribution $n(r)$ curves for a fog density level corresponding to a transmissometer transmittance of approximately 60 percent	31
22.	The size distribution $n(r)$ curves for a fog density level corresponding to a transmissometer transmittance of approximately 90 percent	32
23.	The size distribution $n(r)$ curves for a fog density level corresponding to a transmissometer transmittance of approximately 100 percent	33
24.	Schematic of the cross sections of the laser beam as seen within the aperture of the inlet nozzle on the metal shroud of the ASPS	34

LIST OF TABLES

Table	Title	Page
1.	Numerical Values for Water Droplets Settling in Air	4
2.	Specifications of Active Scattering Spectrometer Probe	24
3.	Calculation of the Volume of the Fog Sample	25

TECHNICAL MEMORANDUM X-64909

THE MEASUREMENT OF THE SIZE-DISTRIBUTION OF ARTIFICIAL FOGS

INTRODUCTION

A program for the measurement of the size-distribution of the fog droplets at the NASA-Ames Research Center fog chamber, located at the University of California (Berkeley) Field Station in Richmond, California, at various fog density levels was performed concurrently, and in connection, with the investigation of the performance of the NASA-Marshall Space Flight Center laser doppler system in artificial fogs.

The measurement of the size-distribution was accomplished by two available methods: (1) the Stokes' velocity photographic method, described in detail in earlier papers [1, 2], and (2) Knollenberg's active particle scattering spectrometer (Particle Measuring Systems Co., Boulder, Colorado) [3]¹ built for the NASA-MSFC Skylab program. Brief descriptions of the two experimental methods are given in a later section.

THE STOKES' VELOCITY PHOTOGRAPHIC METHOD

The details of this method are described in Reference 1. However, a brief description of the photographic system, its principle, and the technique is given below. This technique provides us with a (absolute) method for measuring aerosol size-distributions that is independent of the light-scattering properties of the particles.

The Stokes' Law

The basis of the method is the Stokes' law [4], which relates the terminal velocity (v_s) of a sphere settling freely in a quiet medium to its radius r and is given by the expression

1. Williams, J. R. and Russell, D. M.: Particle Analysis by Active Scattering Particle Spectrometry. Internal unpublished report, NASA-Marshall Space Flight Center, 1973.

$$v_s = \frac{2(\rho_p - \rho_m) g r^2}{9 \eta_m} \quad , \quad (1)$$

where ρ_p and ρ_m represent the specific gravity of the sphere and the medium, respectively, g is the acceleration due to gravity, and η_m is the viscosity of the medium. v_s is also referred to as the Stokes' velocity.

For water droplets ($\rho_p = 1.00$) settling in air ($\rho_m = 1.22 \times 10^{-3}$, $\eta_m = 1.898 \times 10^{-4}$ poise),

$$v_s = 1.22 \times 10^{-2} r^2 \text{ (cm/sec)} \quad . \quad (2)$$

This relation is graphically represented in Figure 1 and the numerical values are given in Table 1.

The Range of Application of the Stokes' Law

Much work has been done to determine the range of application of the Stokes' law. The law is found to be accurate up to a Reynolds number of 0.5. At a Reynolds number of 1, the law is accurate to about 7 percent. At Reynolds numbers above 8, vortex rings form which are stable up to a number of 150, above which the rings become unstable and, from time to time, move off downstream [4].

Several investigators have considered the wall effects for fluid spheres in slow motion [5 - 7]. The investigations were based on Stokes' approximation for the hydrodynamic equations for slow motion. Each assumed a spherical shape is attained for bodies in slow motion [4], and deviation from the spherical shape does not have any noticeable effect on the drag of the fluid body if the ratio of particle diameter to the diameter of the vessel in which the particle is traveling is smaller than 0.5 [8], which is well within the scope of this work. When the diameter of a particle becomes appreciable with respect to the diameter of the container in which it is settling, the container wall will exert an additional retarding effect. This can be compensated for by introducing a factor in the Stokes' equation for frictional drag. Francis [9] has shown experimentally that this correction applies only for values of the diameter ratio less than 0.1. Schiller [10] summarizes correction factors for other than cylindrical boundaries. In general, wall effect correction factors are rarely of

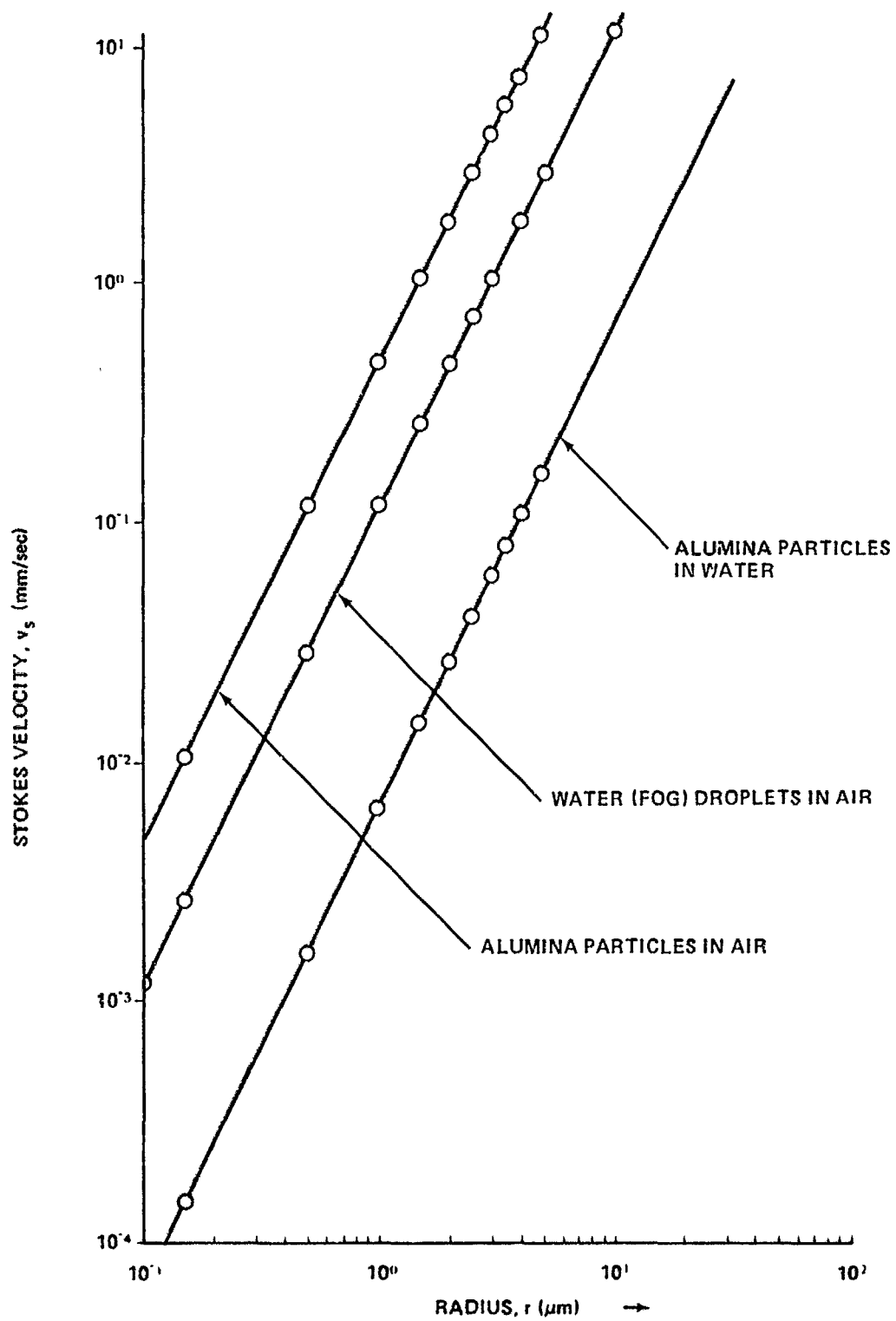


Figure 1. Stokes' velocity versus radius.

TABLE 1. NUMERICAL VALUES FOR WATER DROPLETS SETTLING IN AIR

<p>For water droplets,</p> $\rho_p = 1.0$ <p>For air,</p> $\rho_m = 1.22 \times 10^{-3}$ <p>and</p> $\eta_m = 1.818 \times 10^{-4} \text{ poise (dyne-sec/cm}^2\text{)}$ <p>Droplet radius = r (μm)</p> <p>Stokes' velocity in air,</p> $v_s = 1.2 \times 10^{-1} r^2 \text{ (mm/sec)}$				
Substance of Particles	ρ_p	Radius, r (μm)	Diameter, $2r$ (μm)	Stokes' Velocity, v_s , in Air (mm/sec)
Water	1.0	0.1	0.2	1.20×10^{-3}
		0.2	0.4	4.80×10^{-3}
		0.3	0.6	1.08×10^{-2}
		0.5	1.0	3.00×10^{-2}
		1.0	2.0	1.20×10^{-1}
		1.5	3.0	2.70×10^{-1}
		3.0	6.0	1.08
		4.0	8.0	1.92
		5.0	10.0	3.00
		9.0	18.0	9.72
		10.0	20.0	12.0
		20.0	40.0	48.0
		40.0	80.0	192.0

practical importance when dealing with particles finer than 100 mesh ($147\text{-}\mu\text{m}$ diameter). The largest particle diameter determined in this experiment was $120\text{ }\mu\text{m}$; therefore no wall effect will be included.

Description of the Method

In this method, aerosol particles are allowed to fall freely under gravity in a vertical cell (Fig. 2) in which the convection currents have been reduced to a minimum. The particles are illuminated by a 1-mm thick vertical sheet or slab of light projected into the cell. A camera aimed perpendicular to the slab of light photographs the particle tracks (typical exposure times are 0.5 or 1.0 sec) while the field of view of the lens is chopped at a known rate. The image of the falling particle is thus a series of dashes whose spacing is measured to obtain the settling velocity.

The velocity thus measured is the sum of the Stokes' velocity and the convection velocity. It is the experimental suppression of the convection currents and the theoretical elimination of their effects that is the major cause of the complexity of the experiment and the reason for limiting the method to large particles. The procedures for damping the convection currents are described later.

From prior experience we know that the very small particles of fog ($\sim 1.0\text{ }\mu\text{m}$) move essentially with the convection air currents and, therefore, can be used to measure the vertical component of convection velocities. This component can then be subtracted from the vertical component of the total velocity of large particles to obtain their true Stokes' velocity.

The Experimental Apparatus

The experimental apparatus essentially consists of a vertical cell, an illuminating system, a camera with a bellows, and a uniformly rotating light chopper (Figs. 3 and 4).

The cell is a vertical glass-walled chamber, of octagonal cross-section (each side is $5\text{ cm} \times 45\text{ cm}$), which has airtight joints and can be closed off airtight at the top and bottom (to reduce the air currents). To reduce the initial disturbance inside the cell, a 91 cm (3 ft) high plexiglass extension was placed on top of the chamber. Its walls are covered on the inside with flock paper, except for the appropriate 5 cm diameter openings for the passage of projected

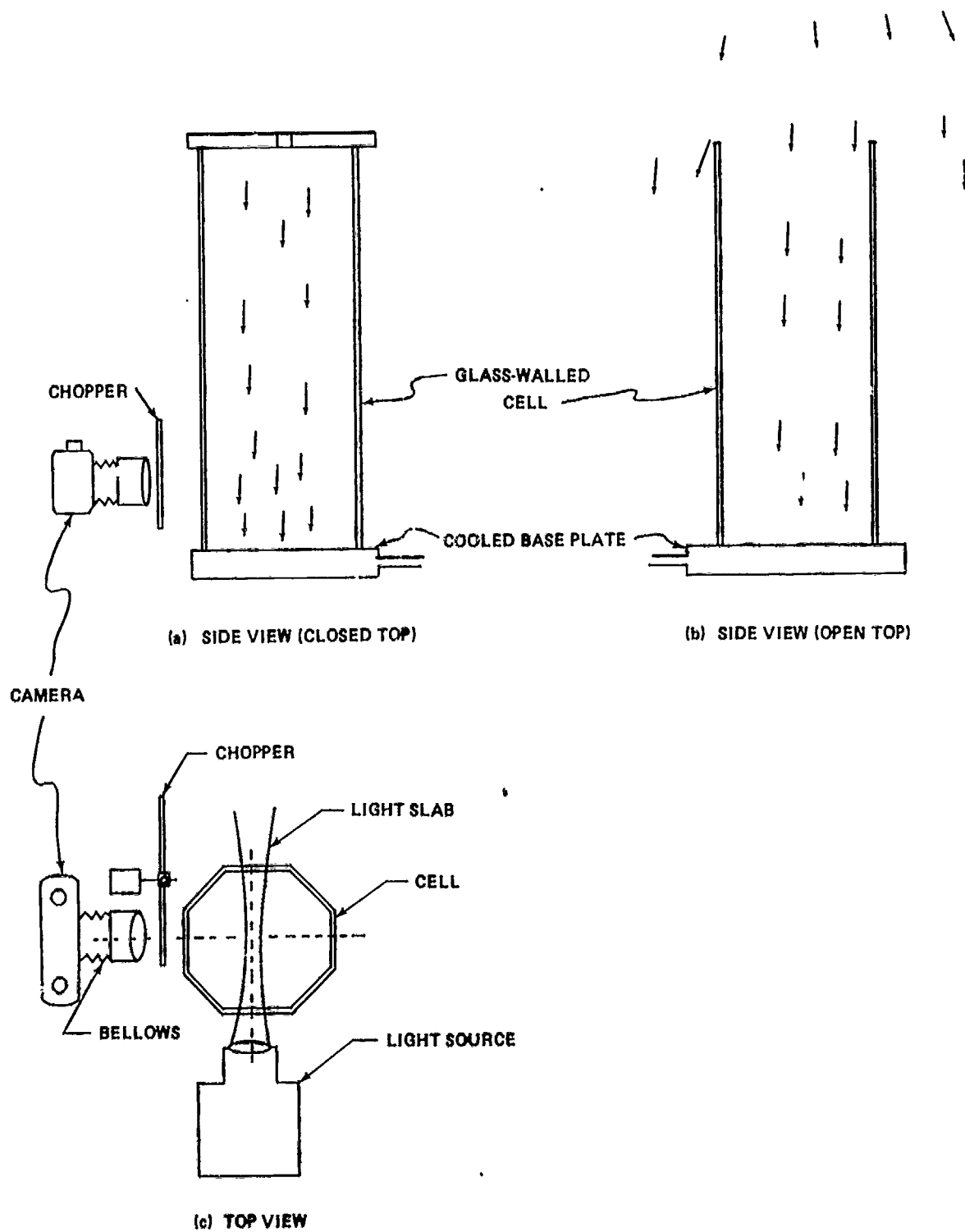


Figure 2. Schematic illustration of the method.

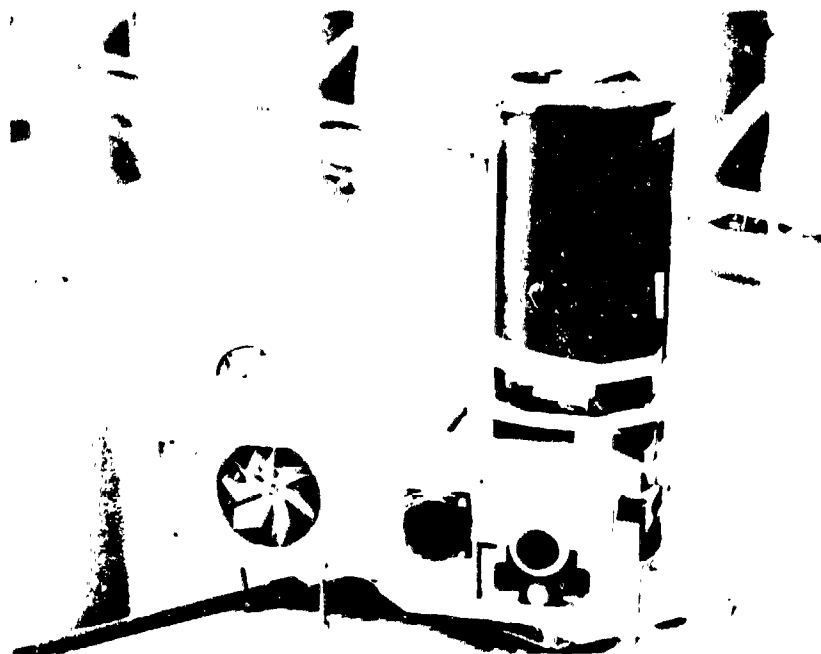


Figure 3. Photograph of the experimental setup.

light and for the camera lens. This helps minimize the extraneous light entering the lens, and provides a dark backdrop for the illuminated particles. The bottom is closed by inserting a 2.5 cm thick aluminum plate which can be cooled to and maintained at the steady temperature of dry ice (-12°C) over its entire surface by circulating a mixture of carbon dioxide dissolved in acetone from a dry ice-and-acetone pump (Fig. 5).

The source of light is a 500-W slide projector (Bell and Howell), with a rectangular aperture ($1\text{ mm} \times 3.81\text{ cm}$) inserted in the position of a slide. The beam of light is projected through a short-focused convex lens ($f/2$) to form a sharp focus of the aperture at the center of the cell. Near the focus a vertical sheet or slab of light 1 mm thick illuminates the falling particles. The depth of focus is approximately 5 mm. The camera unit is an $f/1.7$ Minolta lens mounted in front of a bellows, and the entire unit is fixed to the external framework. The bellows is adjusted to obtain a sharp image of an illuminated object at the position of the projector beam focus, approximately 8.75 cm in front of the lens, so that magnification of nearly unity can be obtained. Typically, the magnification is about 0.8. The camera body can be attached to or removed from the bellows unit for film loading or unloading.

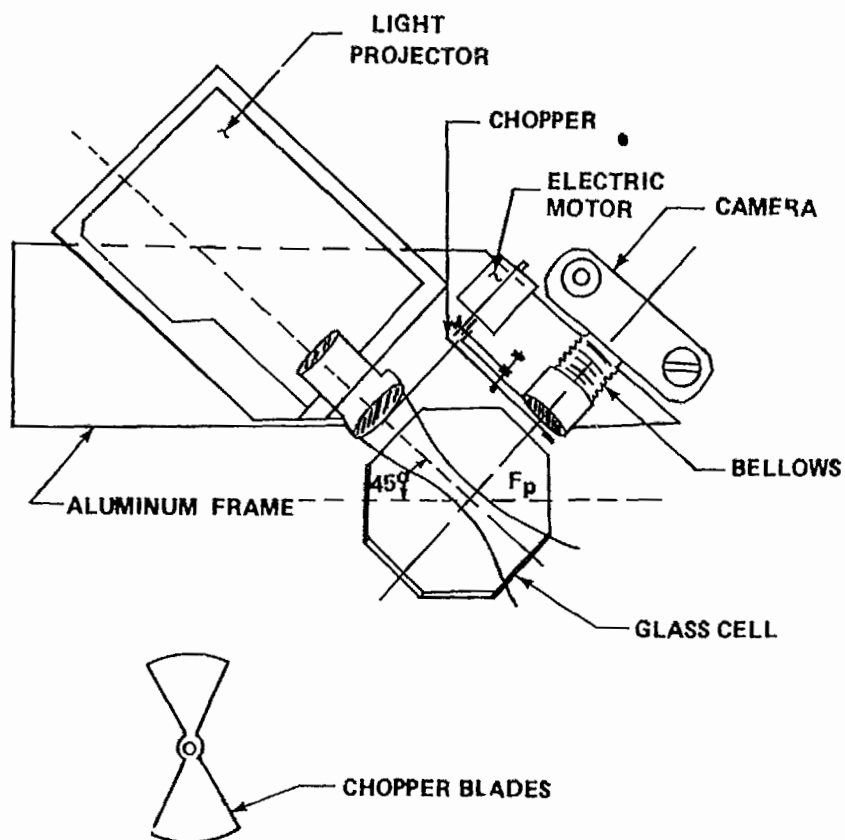


Figure 4. Schematic diagram of the photographic system.

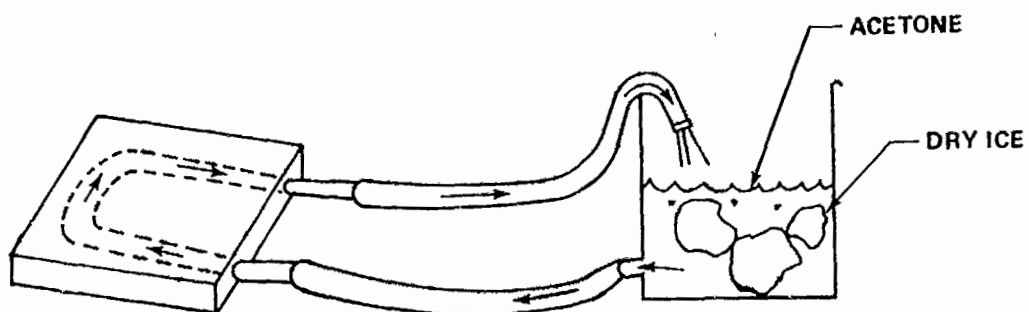


Figure 5. Acetone and dry ice pump.

A uniformly rotating chopper is used just in front of the lens to accurately select and measure the particle track lengths in the photographs. With the help of a belt-and-pully arrangement the chopper (two or four blades) is rotated by a small synchronous electric motor (300 rpm) fixed to the external framework. By choosing an appropriate combination of pulleys and chopper blades, different chopping rates can be obtained (typical values being 10 and 100 chops/sec). In dense fogs (i.e., transmission levels of 1.0 percent and 3.0 percent) the higher speed was used, and in light fogs (transmission levels of 8, 15, 40, and 70 percent) the lower speed was used.

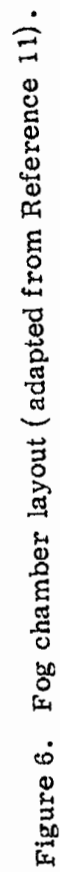
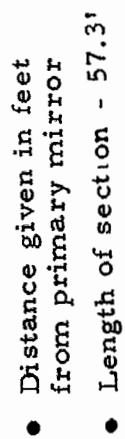
Tri-X (ASA 400) film was found to be the most suitable film because of its speed, resolving power, and ease of developing.

A Settling Experiment with Fog Particles

The measurements of the size distribution of artificial fogs were carried out at the NASA-Ames Research Center fog chamber located at the University of California (Berkeley) Field Station in Richmond, California. The chamber is 305 m (1000 ft) long and 9.5 m (31 ft) wide (Fig. 6). The chamber is divided into 20-m sections which may be filled with fog singly or in combination. The fog is produced by injecting air and water through a series of nozzles at high pressure. During our tests an air/water pressure ratio of 56 248/28 124 kg/m² (80/40 psi) was used. Each section utilizes a transmissometer operating at $\lambda=0.8 \mu\text{m}$ as a sensor to control the fog concentration in that section by a feedback system, which in turn controls the solenoid valves for regulating the water injection. The transmissometer output from all of the working sections feeds to a single counter which gives an average transmittance reading. The 0-percent transmittance level corresponds to about 30.5-m (100-ft) visibility, and 100 percent corresponds to an empty chamber.

The apparatus is placed in the middle of the fogging section for measurement. Some preliminary experimental steps are performed prior to the start of the fog particle measurements.

By letting some fog particles into the cell and with the projector light turned on, several bright specks of light could be seen through the camera viewfinder swirling around as they traversed through the beam. These random flow patterns were created to some extent by the initial disturbance resulting from introducing the particles into the cell and to a large extent by the convection air currents, which arise because of the small differences in the temperatures of the various parts of the cell.



The suppression of these convection currents is essential to the effective working of this method. The most effective procedure for minimizing the convection currents is to cool the bottom plate of the cell. This creates a stabilizing temperature gradient, and consequently density stratification, in the column of air in the cell. The best results were obtained by cooling the plate to a steady temperature of -12°C by a mixture of carbon dioxide dissolved in acetone with the help of the dry ice-and-acetone pump (Fig. 5). The motion of the falling particles was seen to quickly stabilize to a nearly vertical direction of fall within 90 sec after the insertion of particles.

The dry ice-and-acetone mixture was allowed to circulate through the aluminum plate for approximately 30 minutes to insure sufficient cooling of the test section. With the projector light on, a temperature of -23°C (-10°F) was maintained in the optical test section of the cell. To maintain this temperature, it was necessary to turn the projector light off for a few seconds after each photograph. Once cooling was accomplished, the fog generator was turned on and the fog was allowed sufficient time to reach a homogeneous state which was indicated by a digital output of the transmission level in the chamber section in which the apparatus was located (Fig. 7). The top of the cell was opened for a few minutes to enable a sample, containing a sufficient concentration of fog droplets, to enter into the enclosure, and then it was shut airtight.

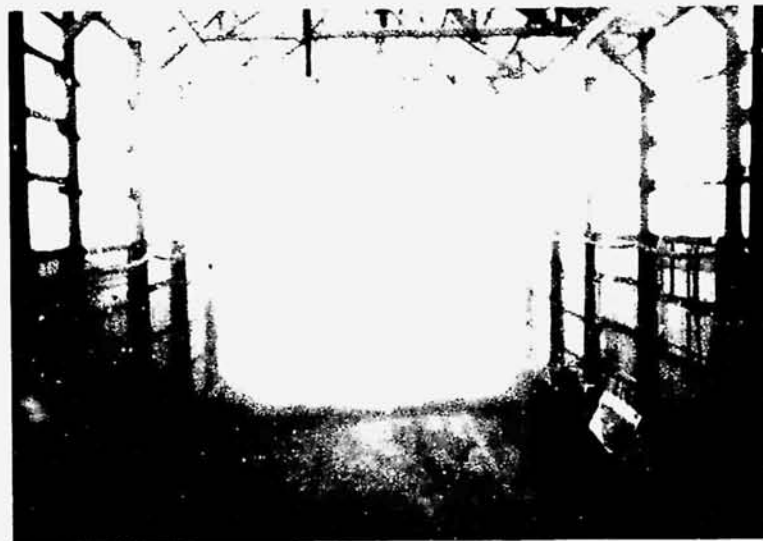


Figure 7. Injection of fog into test chamber.

A series of photographs was taken and developed to determine the quantity of the data. Initially it was found that the light source heated the fog sufficiently to cause fogging of the viewing windows, thus obscuring the photographs. To prevent this, a bottle of nitrogen was obtained, and flow lines were directed over the windows in the plexiglass chamber to prevent clouding of the windows.

It was decided for an adequate statistical average, 1000 particles per fog density level (a fog level being specified by the transmission level) were to be photographed. It was thought that at least 10 particles could be counted in each frame, which meant taking three rolls of film, each roll having 36 exposures. As it turned out, the more dense fogs sometimes produced 40 to 50 particles per frame. However, on this basis, three rolls of film were taken at each different transmission level (1, 3, 8, 15, 40, and 70 percent) with the photographs being taken 12 at a time with a short interval between each picture so that each fog was photographed 108 times.

The following experimental steps and measurements were taken to ensure good accuracy of the results:

1. The camera lens and the glass walls of the cell were periodically checked for fogging. Fogging was cleared by using a fine jet of nitrogen gas from a bottle.
2. The cell was airtight. This was checked before the experiment by means of a water leakage test.
3. The cool bottom plate was kept as close as possible to the level of the measuring optics (about 3.0 cm) because the stabilization of the convection currents is maximum near the cooling plate.
4. A check for any noticeable effects of coagulation or evaporation of fog particles during the fall through the chamber was also made.
5. The instrument was kept away from the direct line of squirting fog jets from the nozzles in the fog chamber.
6. The temperature of the air at the levels of the measuring optics was taken to obtain the exact value of the air viscosity (η_{air}) from tables.
7. The measurement of the particle track lengths on the photographs was made with an automated track-length analyzer. The output is in the form of punched computer cards.

8. For transmission levels of 1 percent or 3 percent, an appropriate combination of chopper blades and pulleys was used to obtain 100 chops/sec; for low density fogs, 10 chops/sec was sufficient.

9. The following quantities were also checked for their accuracy:

- a. Camera shutter speed.
- b. Chopper speeds (two or four blade).
- c. Photographic track analyzer scale.
- d. Magnification factor.
- e. Area of cross section and volume of the sampled section of the beam.

Experimental Measurements and Results

Camera Shutter Speed. The camera shutter speed was checked by putting a photodiode in the plane of the film and measuring the duration of the 1.0-sec exposure with an oscilloscope. The oscilloscope photograph (Fig. 8) shows that for a shutter speed of 1.0 sec, the time exposure interval, T_{exp} , is 1.2 sec.

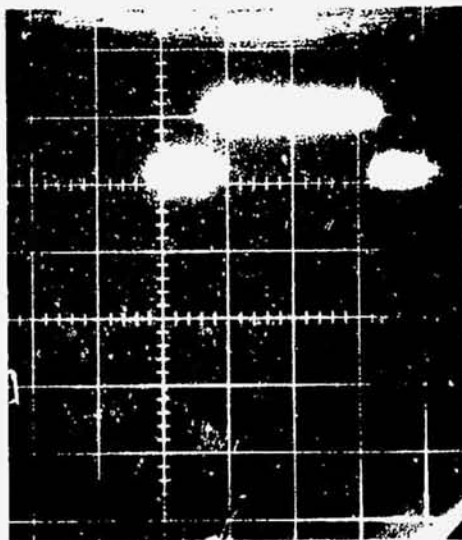


Figure 8. Oscilloscope photograph (time scale: 1 cm = 0.5 sec).

Chopper Speeds (For Dense and Light Fogs). The path of the light beam incident on the photodiode was chopped and the rate of chopping was measured by the chart recorded. For light fogs a two-blade chopper was used with its pulley diameter of such a size as to give about 10 chops/sec. For dense fogs ($T \leq 3$ percent) the two-blade chopper can be replaced by a four-blade chopper with its pulley diameter of such a size as to give about 100 chops/sec. The exact rate was measured from the chart recorders (Fig. 9) to be: for light fogs ($T > 3$ percent),

$$R_c = 12.5 \text{ (chops/sec)} \quad ; \quad (3a)$$

for dense fogs ($T \leq 3$ percent),

$$R_c = 81.5 \text{ (chops/sec)} \quad . \quad (3b)$$

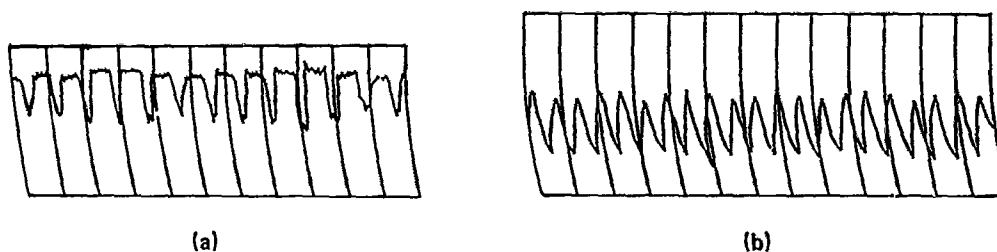


Figure 9. The chopping rate recorded on a chart recorder for: (1) a small pulley and two-blade chopper (chart speed = 5.0 cm/sec) and (2) a large pulley and a four-blade chopper (chart speed = 25.0 cm/sec).

Photographic Track Analyzer (PTA) Instrument Calibration Constants
 (C_x, C_y) . The calibration constants for the PTA instrument for the x- and y-axes are:

$$C_x = 1/2796.38 \text{ (cm/unit)}$$

and

$$C_y = 1/2815.8 \text{ (cm/unit)} \quad .$$

Magnification Factors, M. The linear magnification is

$$M = \text{Image Size/Object Size} \quad .$$

The magnification can be varied with the help of the bellows by proper positioning of the camera lens between the object plane and the film plane. Millimeter graph paper was attached to the end of a meter stick and lowered into the center plane of the projected sheet of light and photographed (Fig. 10). The linear magnification, M_y , along the y-direction was calculated to be approximately 0.788. The magnification along the x-direction was the same.

Area of Cross Section and Sampled Volume. The horizontal beam cross section was obtained by placing a sheet of paper horizontally in the middle of the beam and measuring the dimensions of the illuminated portion. The shaded parts (Fig. 11) represent the cross-sectional area intercepted by the view cone of the lens.

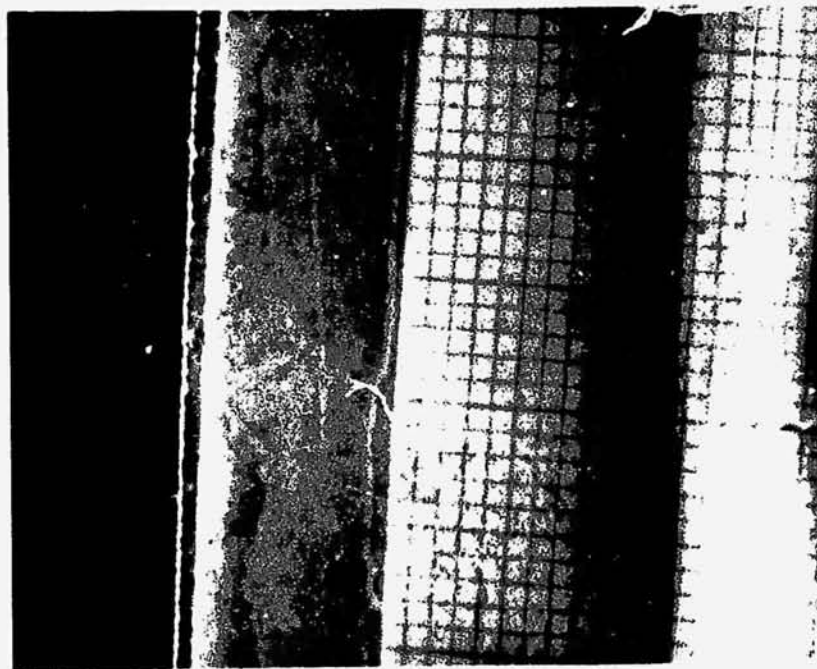


Figure 10. A photograph of the graph paper scale placed in the center plane of the slab of light.

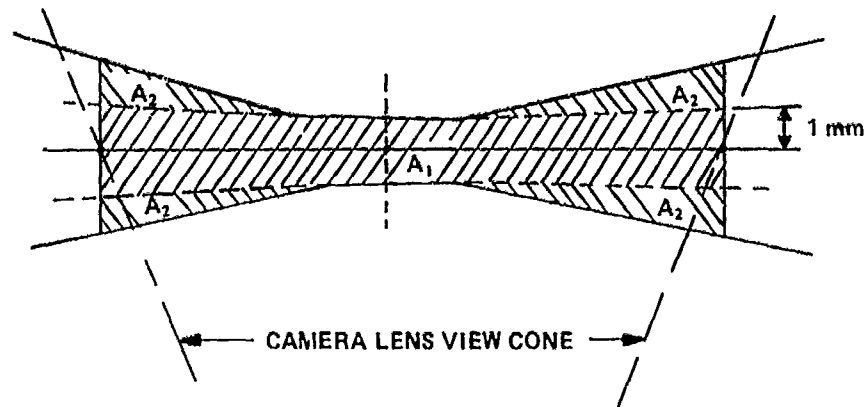


Figure 11. Schematic of the horizontal cross section of the projected sheet of light.

The total area of the cross section is

$$A = A_1 + 4 A_2 = 1.084 \text{ cm}^2 \quad .$$

The height of the beam is

$$h = 3.046 \text{ cm} \quad .$$

Then the illuminated volume seen by the lens is

$$V_L = A \times h = 3.301 \text{ cm}^3 \quad .$$

However, we find from experimental tests that the depth of focus of the camera lens is

$$d = 0.2 \text{ cm} \quad .$$

Since only the relatively sharply focused tracks are used in the measurements, the area of the cross section is

$$A = 0.91 (d \times 3.6/M) \text{ cm}^2 ,$$

and the volume of sampled particles is

$$V = hA = (2.4/M) A = 2.73 \text{ cm}^3 . \quad (4)$$

Measurement of Track Lengths. The photographs (such as in Fig. 12) were processed by the Photographic Laboratory of Marshall Space Flight Center. Each photograph contained approximately 4 to 10 particles for light fogs and more than 10 particles for dense fogs. Each particle is represented by a dashed line, with the length of each dash being an indication of the velocity of a particular particle. The length of each dash or track was determined by the use of a photographic track analyzer instrument which produced a punched computer card. It was necessary to visually locate the beginning and ending of each dash per particle which was automatically recorded on a computer card, one measurement per card.

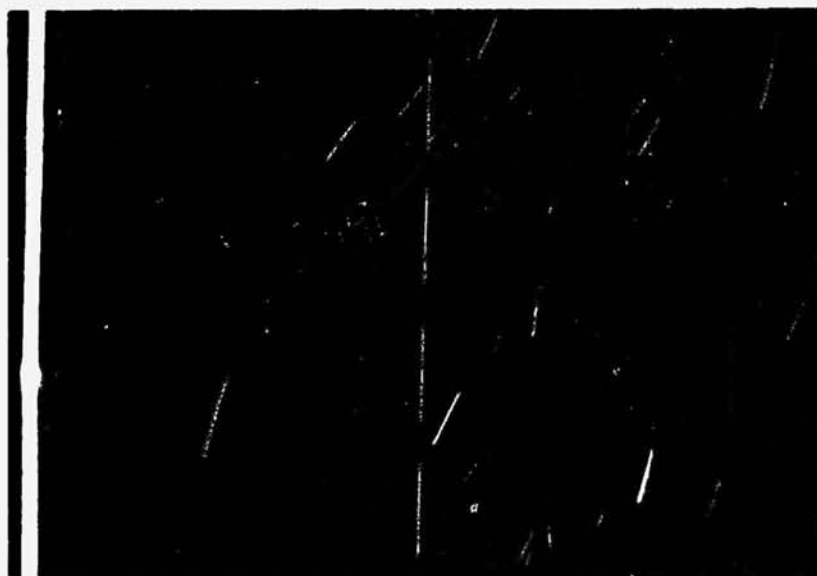


Figure 12. A typical photograph of fog particles inside the chamber.

Data Analysis

Radius from Particle Tracks. From the Stokes' law, the radius of a fog droplet settling under gravity in quiet air with a velocity v_s (cm/sec) is

$$r = 0.09125 (v_s)^{1/2} \text{ (cm)} \quad (5)$$

Let, h'_x, h'_y (in instrument units) and h_x, h_y (in cm) represent the x- and y-components of the complete track length for those tracks (represented by "IN") that are fully within the photograph, and the components of the length of a single dash for those tracks (represented by "OUT") that either end or start within the photograph. Also, let t_y be the time of travel of the particle in seconds.

$$h_y = \left(\frac{h'_y C_y}{M_y} \right) \quad (6)$$

where M_y is the magnification factor and C_y is a calibration constant. For IN-track,

$$t_y = T_{\text{exp}} \quad (7a)$$

where T_{exp} is the exposure time. For OUT-track,

$$t_y = 1/R_c \quad (7b)$$

where R_c = chops per second. The vertical velocity is

$$v_y = h_y / t_y \quad (8)$$

From prior experience with DOP particles [1] we know that the air currents inside the chamber near the optical test section have a vertical velocity component,

$$v_c \approx 0.1 \text{ cm/sec} \quad (9)$$

Then the Stokes' velocity of the particles is

$$v_s = (v_y - v_c) \quad (10)$$

Substitute this value into equation (5) to obtain r .

The Particle Size Distribution, $n(r)$. To analyze the data, the particle tracks in a number of photographs are measured and reduced to particle velocity (and consequently particle radius). To obtain a 10-percent error bar in each of the 10, for example, particle radius intervals, it is necessary to reduce about 1000 tracks (± 20 percent in 10 intervals requires about 250 tracks).

If the particle tracks are all entirely contained within the viewed volume, the average particle size distribution can be evaluated as shown below.

The height of the viewed region = h .

The area of the horizontal cross section viewed region = A .

The volume of the viewed region = hA .

If $N_p(r_i, \Delta r)$ is the number of particles seen in the p th photograph for which the particle radius lies between $r_i - \Delta r/2$ and $r_i + \Delta r/2$ and N_f is the total number of frames viewed, then the size distribution for the i th radius interval is given by

$$[n(r)]_i = \frac{1}{N_f} \sum_p \left[\frac{N_p(r_i, \Delta r)}{hA \Delta r} \right] \quad (11)$$

$$[n(r)]_i = \frac{1}{N_f h A \Delta r} \sum_p N_p(r_i, \Delta r) \quad (12)$$

if h , A , and Δr are constant.

For particles whose tracks do not originate and/or terminate in the illuminated volume, the procedure is to count the number of tracks, $N_p(r_i, \Delta r; z_j)$, which pass through a given elevation z_j in the cell during the exposure time. If measurements are made at the number (N_z) of levels in the photograph, then the particle size distribution in this case is given by

$$[n(r)]_i = \frac{1}{N_f N_z} \sum_p \frac{N_p(r_i, \Delta r; z_j)}{[v_s(r_i) \Delta t_p] A \Delta r} \quad (13)$$

where $v_s(r_i)$ is the velocity and Δt_p is the exposure time. $N_p(r_i, \Delta r; z_j)$ is the number of particles crossing lines at each of the z_j levels, regardless of whether the same particle has been counted on other levels.

ACTIVE SCATTERING PARTICLE SPECTROMETER (ASPS) METHOD [3]

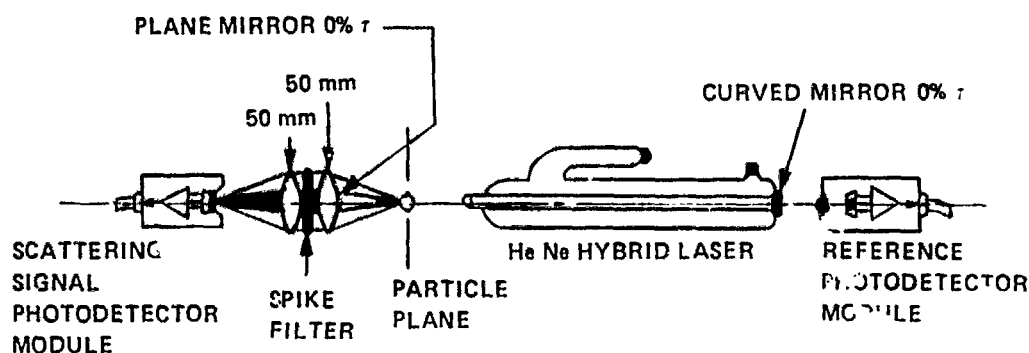
Description of the Instrument²

The active scattering particle spectrometer (ASPS) was custom designed under NASA contract for the Skylab Contamination Ground Test Program (SCGTP) by Dr. Robert Knollenberg [3] of Particle Measuring Systems Co., Boulder, Colorado, to measure particle size-distributions and velocities for particles in the size range of $0.1 \mu\text{m}$ to $29 \mu\text{m}$ with a velocity detectability from 0.1 m/sec to 50.0 m/sec .

Figure 13 is a schematic of the optical system of the ASPS. The light source is an He-Ne laser operating in the IEM mode. One of the laser mirrors is cemented to the plasma tube. The light "leakage" through this mirror is

2. Ibid.

ACTIVE SCATTERING AEROSOL SPECTROMETER OPTICAL SYSTEM
FOR 0.1 TO 1.5 μm AEROSOL SIZE RANGE



NOTE: MIRRORS REVERSED FOR 1 TO 25 μm RANGE

Figure 13. Optical system diagram for active scattering particle spectrometer.

monitored with a photodetector and serves as a reference, therefore any changes in the laser are balanced onto the other output. The other laser mirror is cemented to a lens. The particle sample plane is now in the laser cavity, and the mirror serves as the block for the collimated or unscattered light. The scattered light is collected by the lens system and directed to a photodetector. Again, the scattered light intensity is proportional to the particle size. By working in the laser cavity instead of outside it, one can get as much as two orders of magnitude increase in available light.

To cover the size range from 0.1 μm to 29 μm the ASPS probe actually consists of two intercavity lasers in one housing. The only difference between the two lasers is in the sample volume. This is accomplished by placement choice on the laser mirrors. The unit covering the range from 0.1 μm to 1.5 μm has the spherical mirror on the plasma tube and the plane mirror on the collection lens, as shown in Figure 13. This means that the laser beam is focused down as it passes through the sample volume, thus producing a relatively small sample volume. The unit covering the range from 1 μm to 29 μm has the mirrors reversed. The laser beam is larger in the sample region with this configuration. In the 0.1 μm to 1.5 μm range the sample volume is a cylinder 210 μm in diameter by 8 mm, while in the 1 μm to 2 μm range the sample volume is a cylinder 1.5 mm in diameter by 8 mm.

Figure 14 is a photograph of the ASPS probe. It is a stainless steel cylinder 16 cm in diameter with a total length of approximately 85 cm. The laser tubes and electronics are sealed in the body of the stainless steel housing.

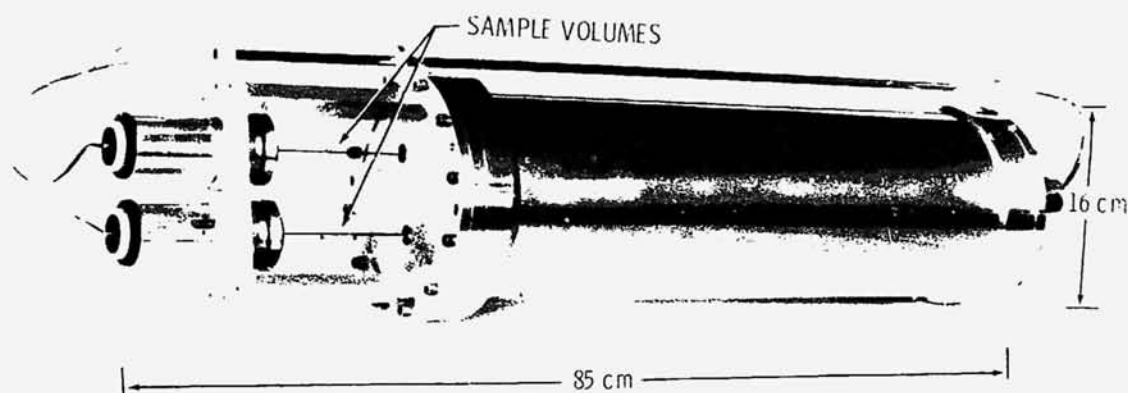


Figure 14. Active scattering particle spectrometer probe.

allowing the probe to operate from ambient conditions to ultrahigh vacuum conditions. The external laser mirrors, collection lenses, and detectors are mounted on an extension of the metal cylinder. The area between this mount and the cylinder is within the laser cavities, as indicated by the sample volumes. The ASPS can measure particles that "free flow" through the cavity. Metal shrouds with tubing can be inserted around the laser beams and air pulled through the cavity with a small vacuum pump.

Figure 15 is a photograph of the data system and control console for the ASPS. As can be seen in the photograph each laser unit has independent control and data readout. The CRT's display the real time histogram with particle size on the horizontal axis and particle count on the vertical axis. With the channel thumbwheel and particle count indicator one can monitor a specific size growth or manually dial through the histogram.

The specifications of the ASPS are given in Table 2.

Particle Size Distribution, $n(r)$

The air at a slow known rate of 1.4 liters/min is drawn through a tube so that fog particles pass through the two focal volumes in succession. The air is allowed to flow through the metal shrouds for a minute or so until a relatively large reading on the channel counters is registered. The digital readout N_i of each of the 15 channels ($i = 1, 15$) in counters No. 1 and No. 2



Figure 15. Active scattering particle spectrometer data system and control console.

can then be divided by the sample volume V (Table 3) and by the radius interval Δr to obtain the size distribution,

$$n(r) = \frac{1}{N} \sum_{i=1}^{15} \frac{N_i}{V \Delta r_i} \quad (\text{cm}^{-3} \mu\text{m}^{-1}) \quad ,$$

DISCUSSION OF THE RESULTS

The $n(r)$ versus r curves as obtained from the two methods are plotted in Figures 16 through 23 for different levels of the fog densities in the fog chamber. The figures show that the Knollenberg probe yields a more accurate measurement of the fog particle size-distribution, $n(r)$, than the Stokes' velocity method for particles of radii less than 10 to 12 μm , while the reverse is true for larger particles. Preliminary calculations show that the contribution to the

TABLE 2. SPECIFICATIONS OF ACTIVE SCATTERING SPECTROMETER PROBE

	Counter 1		Counter 2	
	15		15	
Number of Size Channels	0.1 to 1.5 μm		1 to 23 μm	
Size Range	0.1 μm		1.0 μm	
Minimum Detectable Size	Varies with size		Varies with size	
Size Resolution	250 kHz		25 kHz	
Maximum Particle Rate	Less than 1 percent with concentrations of 10^3 cm^{-3} .		Less than 1 percent with concentrations of 10^2 cm^{-3} .	
Coincidence Errors	50 m sec^{-1}		50 m sec^{-1}	
Maximum Particle Velocity	RMS size errors: ± 10 percent or $\pm 0.1 \mu\text{m}$, whichever is greater. Velocity error ± 10 percent.		RMS size errors: ± 10 percent or $\pm 1.0 \mu\text{m}$, whichever is greater. Velocity error ± 10 percent.	
Accuracy				
<u>General Specifications</u>				
Power	115 V, 60 Hz; 0.5 A, 55 W			
Dimensions	Cylinder: 71.12 cm (28 in.) long, 16.5 cm (6.5 in.) in diameter			
Weight	13.6 kg (30 lb)			

TABLE 3. CALCULATION OF THE VOLUME OF THE FOG SAMPLE

	Counter No. 1 (0.1 μ m to 1.5 μ m)	Counter No. 2 (1.0 μ m to 29 μ m)
Laser beam, d_b (Fig. 24)	0.0256 cm	0.17 cm
Inlet Nozzle, d_{noz}	0.1875 in. = 0.476 cm	0.476 cm
Beam Area, A_{beam}	$d_b \times d_{noz} = 0.0256 \times 0.476$	0.17×0.476
Nozzle Area, A_{noz}	$\frac{\pi}{4} \times (d_{noz})^2 = \frac{\pi}{4} (0.476)^2 = 0.178 \text{ cm}^2$	0.178 cm^2
Flow Rate	1.4 LPM = 1400 cm^3/min	1.4 LPM = 1400 cm^3/min
Velocity, V_N	$\frac{\text{Flow Rate}}{A_{noz}} = \left(\frac{1400}{0.178} \right) \frac{\text{cm}}{\text{min}}$	$\frac{1400}{0.178} \frac{\text{cm}}{\text{min}}$
Volume of Fog Sampled, V	$A_{beam} \times V_N \times \text{time}$	

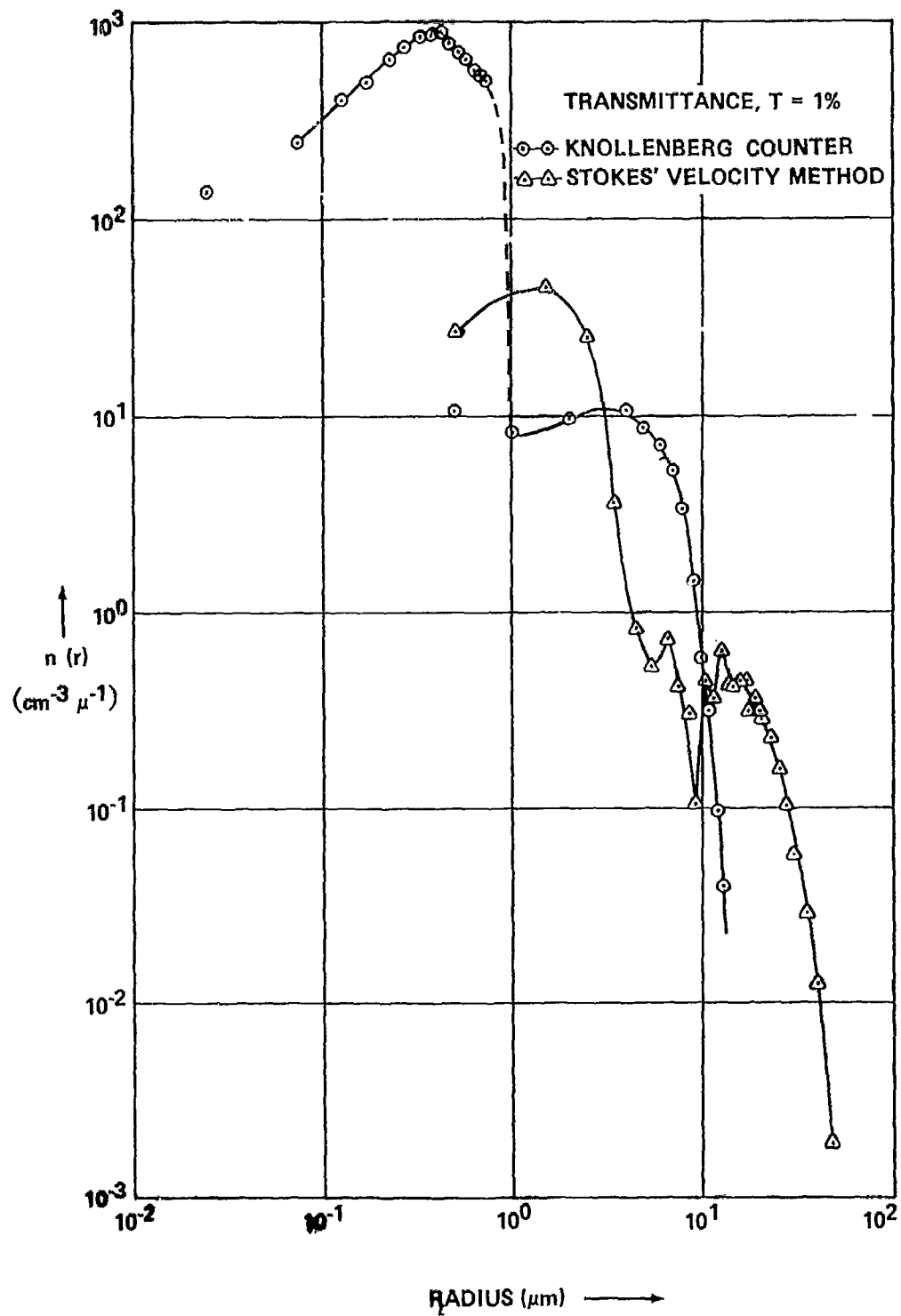


Figure 16. The size distribution $n(r)$ curves for a fog density level corresponding to a transmissometer transmittance of approximately 1 percent.

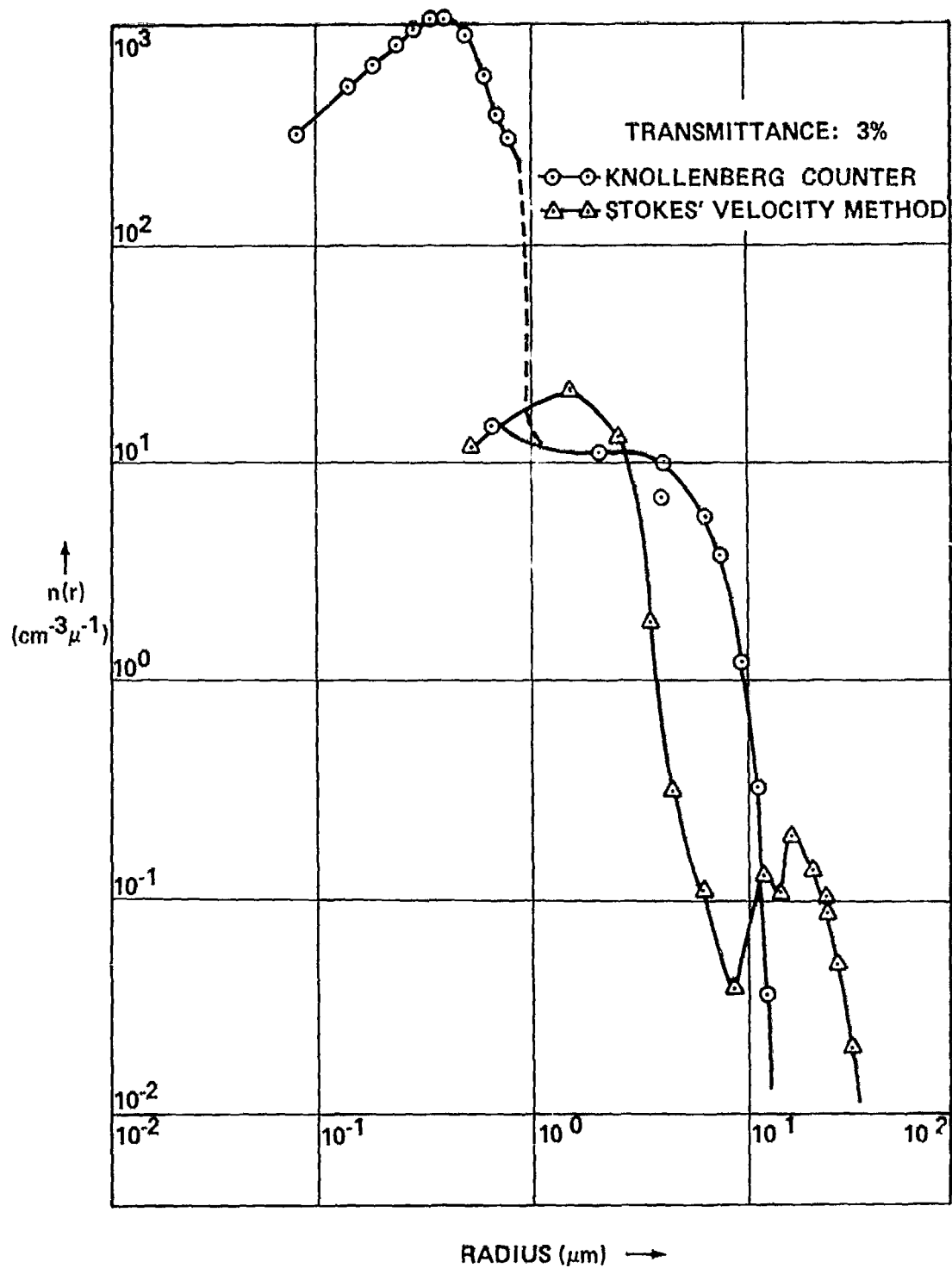


Figure 17. The size distribution $n(r)$ curves for a fog density level corresponding to a transmissometer transmittance of approximately 3 percent.

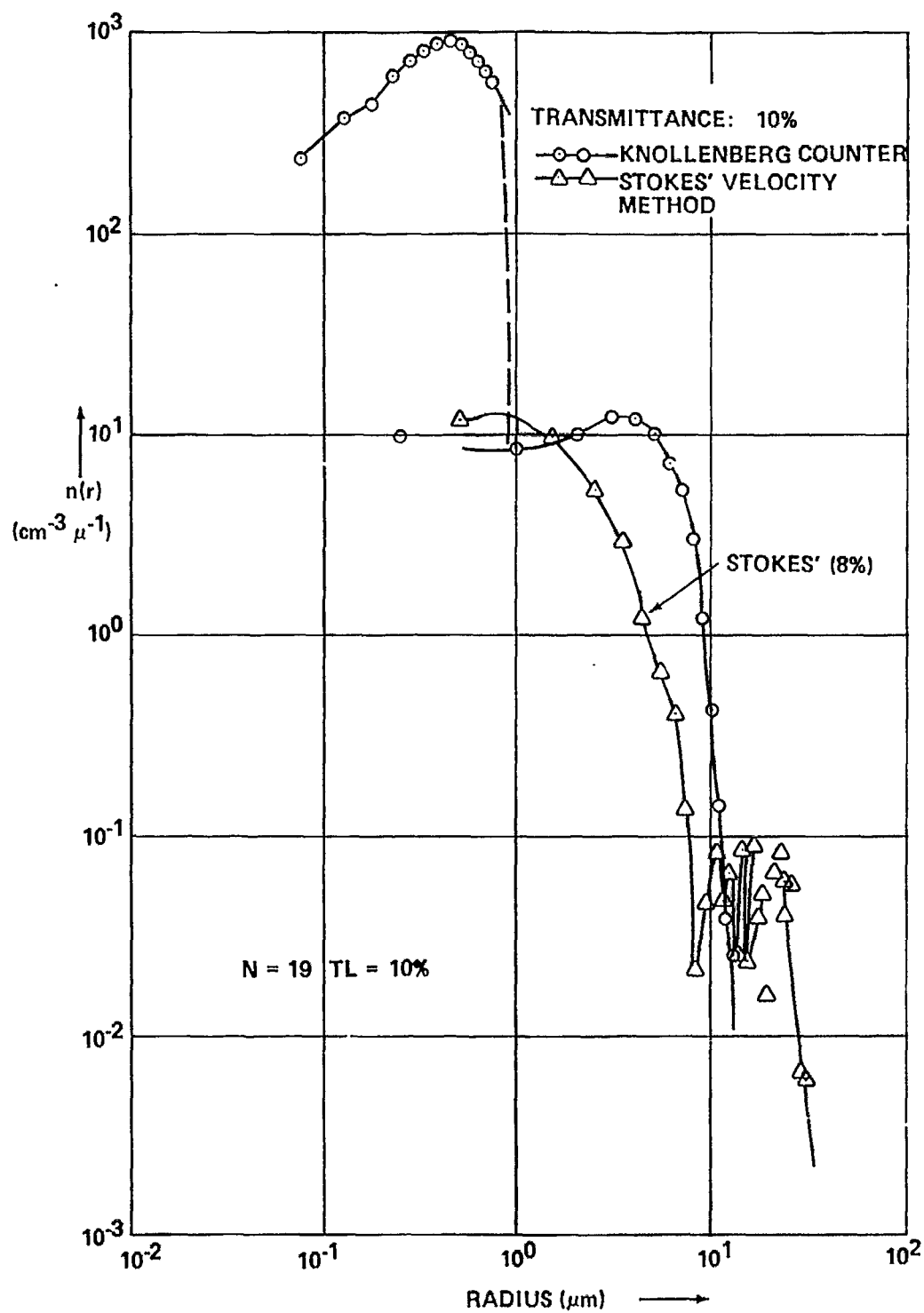


Figure 18. The size distribution $n(r)$ curves for a fog density level corresponding to a transmissometer transmittance of approximately 10 percent.

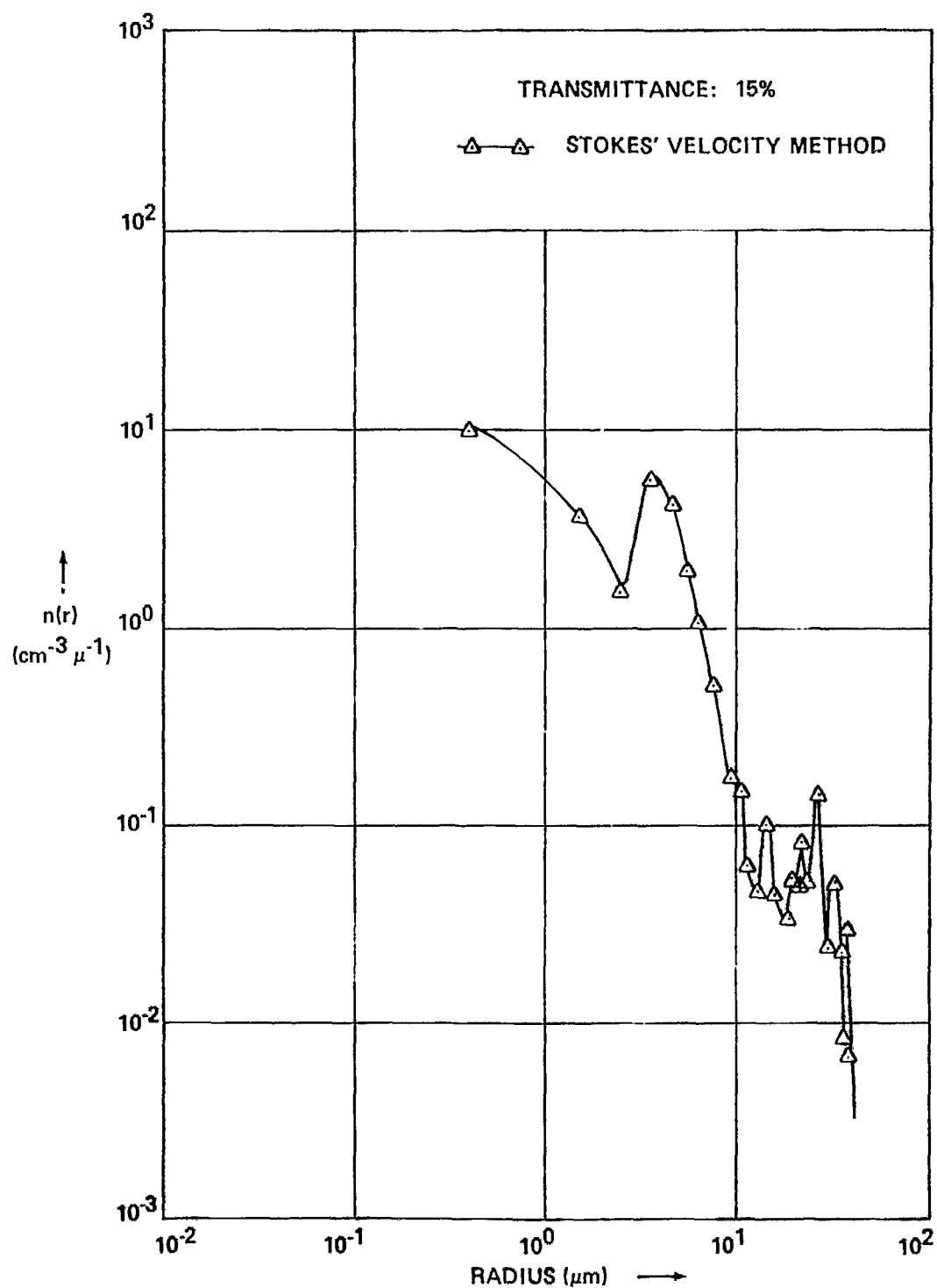


Figure 19. The size distribution $n(r)$ curves for a fog density level corresponding to a transmissometer transmittance of approximately 15 percent.

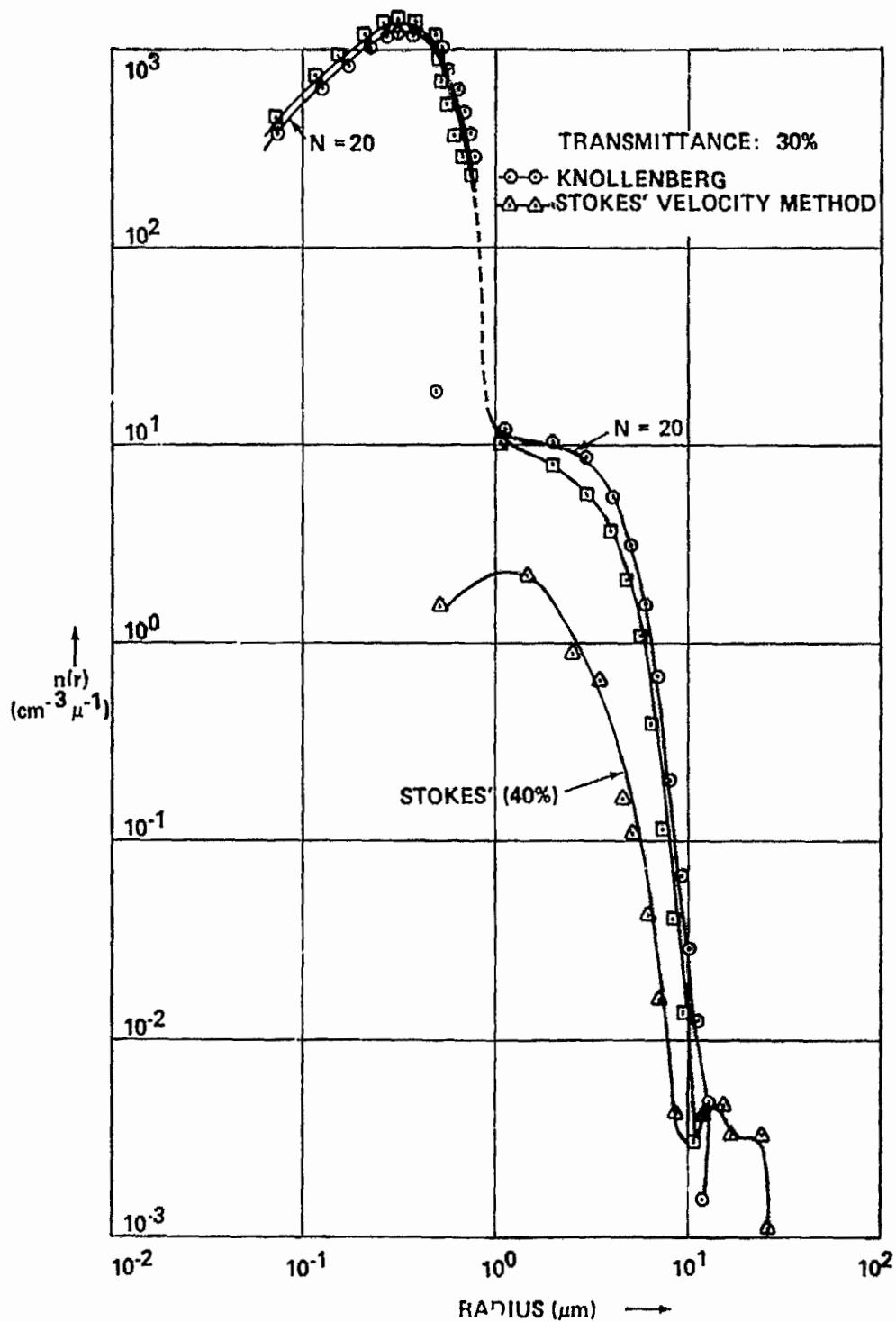


Figure 20. The size distribution $n(r)$ curves for a fog density level corresponding to a transmissometer transmittance of approximately 30 percent.

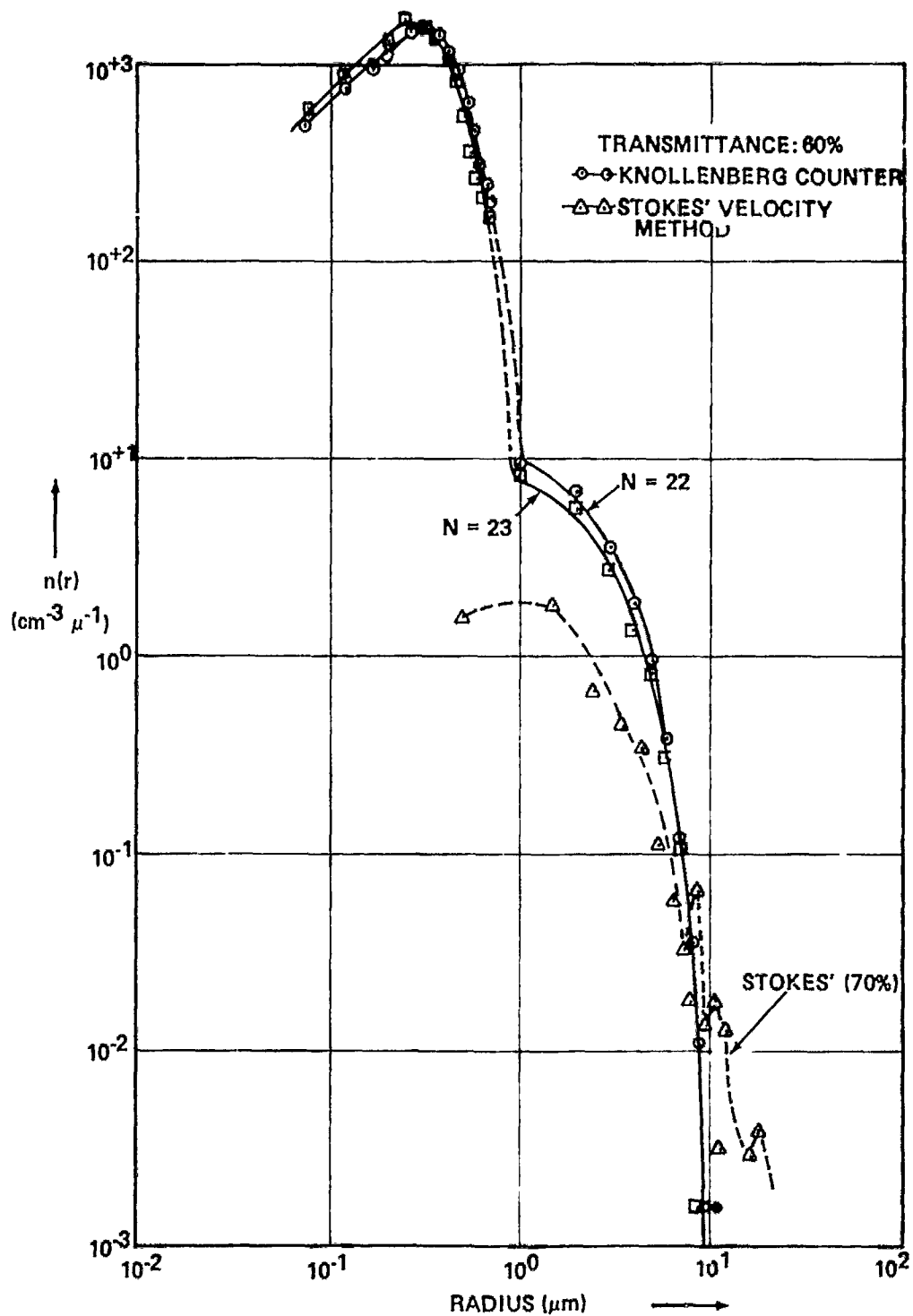


Figure 21. The size distribution $n(r)$ curves for a fog density level corresponding to a transmissometer transmittance of approximately 60 percent.

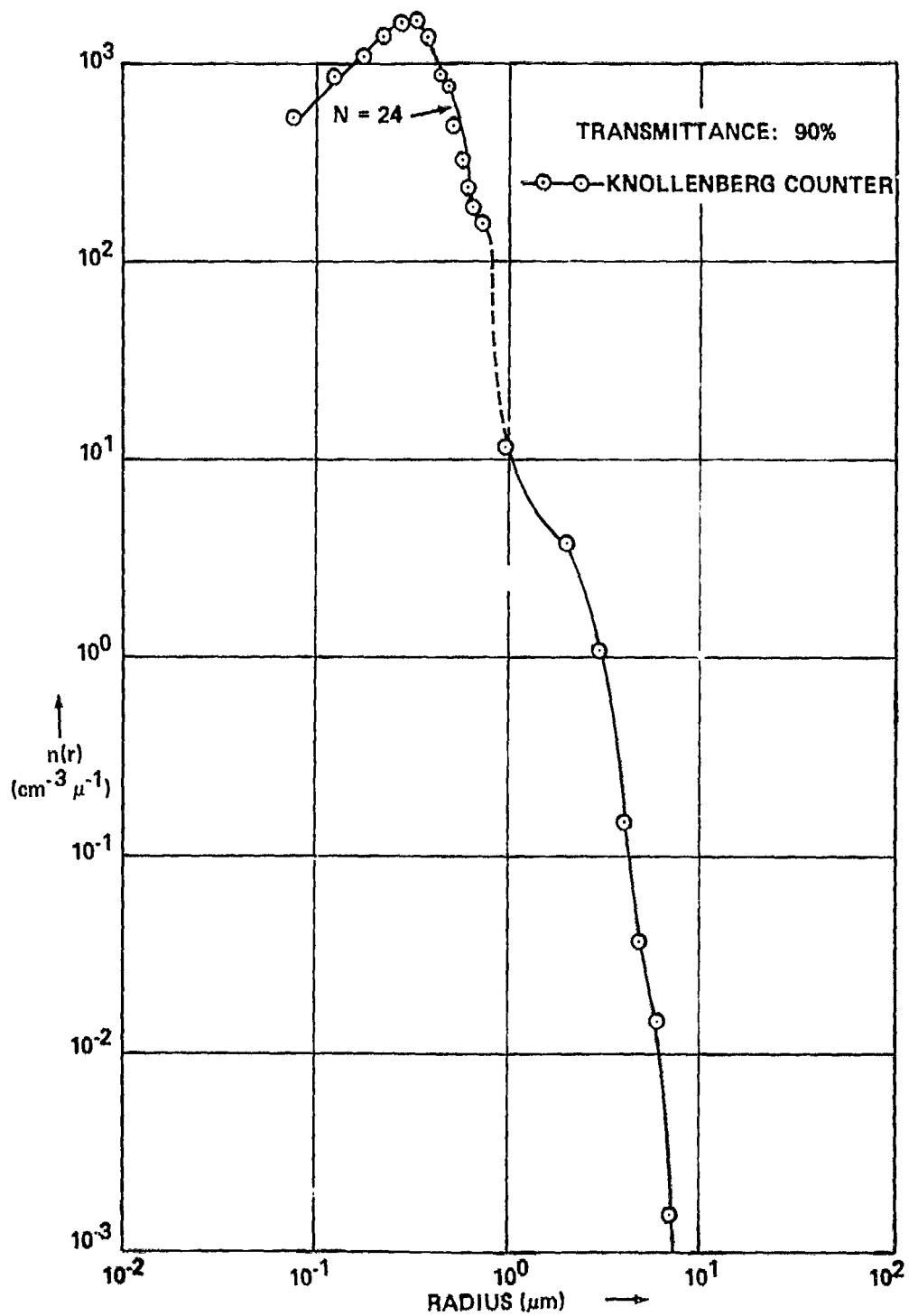


Figure 22. The size distribution $n(r)$ curves for a fog density level corresponding to a transmissometer transmittance of approximately 90 percent.

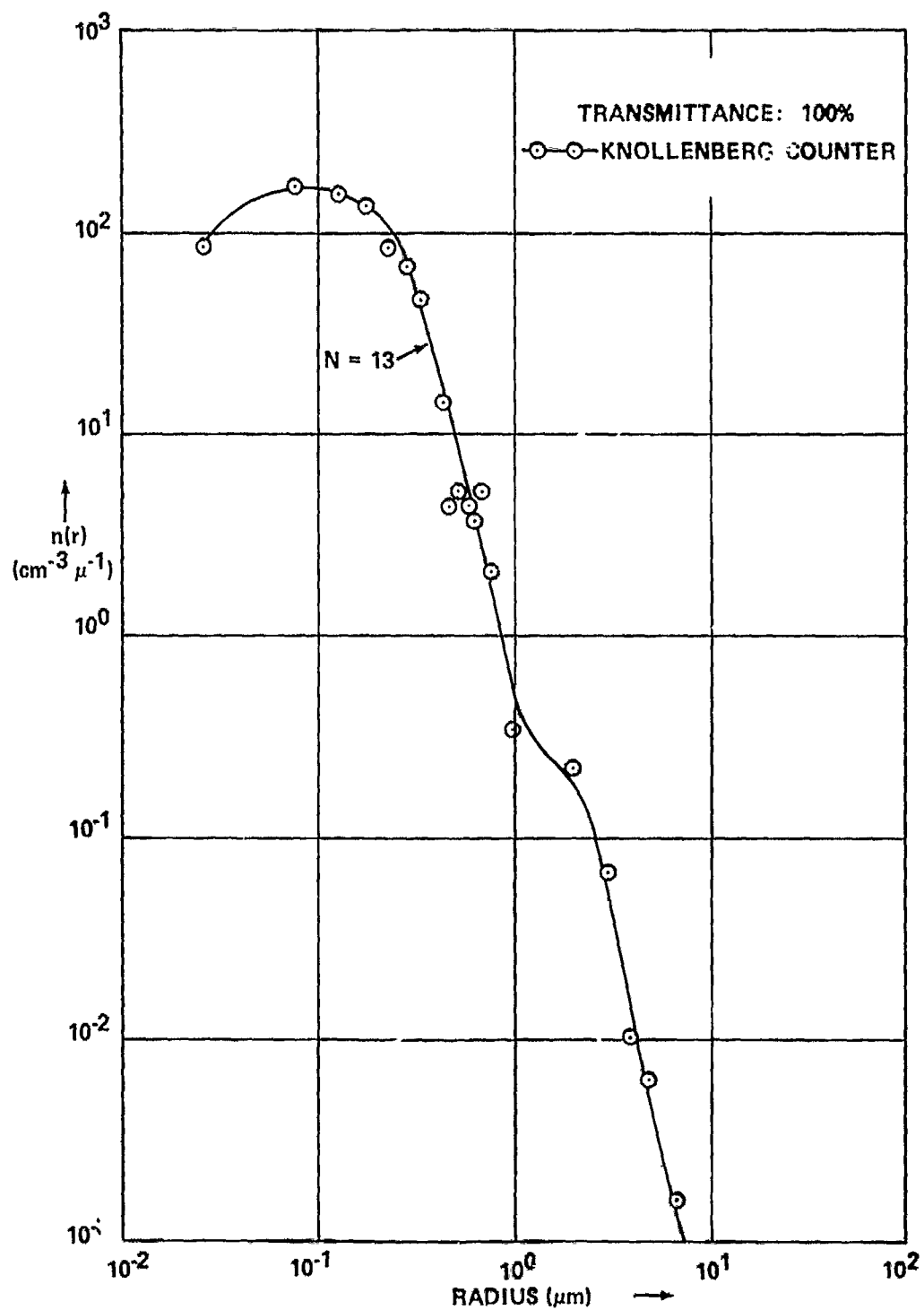


Figure 23. The size distribution $n(r)$ curves for a fog density level corresponding to a transmissometer transmittance of approximately 100 percent.

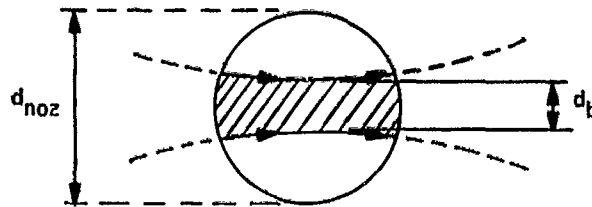


Figure 24. Schematic of the cross sections of the laser beam as seen within the aperture of the inlet nozzle on the metal shroud of the ASPS.

volume scattering coefficient, β_e , and to the backscattering function, $\beta(\pi)$, of the small number of large size particles (radius greater than $12 \mu\text{m}$) is larger than or comparable to that of the very large number of smaller size particles (radius less than $10.0 \mu\text{m}$) for the IR radiation, such as the $\lambda = 10.6 \mu\text{m}$ radiation. Hence it is important to measure the very large fog particles (radius greater than $12 \mu\text{m}$), for which the Stokes' velocity method is accurate to an adequate degree [1].

REFERENCES

1. Deepak, A.: A Stokes' Velocity Photographic Method for Measuring the Size Distribution of Aerosols. NASA TM X-64838, 1974.
2. Deepak, A., et al.: A Standard Particle Sizer-Velocimeter. NASA TM X-64857, 1974.
3. Knollenberg, R. G.: An Active Scattering Across Spectrometer. Atmospheric Technology, vol. 2, June 1973, pp. 80-81.
4. Stokes, G. G.: Trans. Cambridge Phil. Soc., vol. 9, no. 8, 1851.
5. Brenner, H.; and Happel, J.: Journal of Fluid Mechanics, vol. 4, 1958, p. 195.
6. Brenner, H.: Journal of Fluid Mechanics, vol. 12, 1962, pp. 35-48.
7. Taylor, T. D.; and Acrivos, A.: Journal of Fluid Mechanics, vol. 18, 1964, pp. 466-467.
8. Lapple, C. E.: Fluid and Particle Mechanics. University of Delaware, Newark, Delaware, 1965.
9. Francis, A. W.: Physics, vol. 4, 1933, pp. 403-406.
10. Schiller, L.: Handbuch der Experimentalphysik. Vol. IV, Part 2, Leipzig, Akademische Verlagsgesellschaft, 1932, pp. 337-387.
11. Lawrence, T. R., et al.: Lockheed/Huntsville Engineering Report, LMSC-HREC-TRD306888(1973), under Contract NAS 8-29606.


APPROVAL

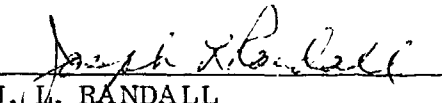
THE MEASUREMENT OF THE SIZE-DISTRIBUTION OF ARTIFICIAL FOGS

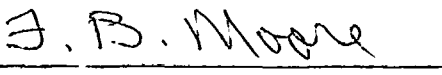
By Adarsh Deepak, William C. Cliff, John R. McDonald,
Robert Ozarski, J. A. L. Thomson, and Robert M. Huffaker

The information in this report has been reviewed for security classification. Review of any information concerning Department of Defense or Atomic Energy Commission programs has been made by the MSFC Security Classification Officer. This report, in its entirety, has been determined to be unclassified.

This document has also been reviewed and approved for technical accuracy.


E. J. REINBOLT
Chief, Laser Engineering Branch


J. L. RANDALL
Chief, Optical and R. F. Systems Division


F. B. MOORE
Director, Electronics and Control Laboratory